

Bridging scales in multiphysical VCSEL modeling

Original

Bridging scales in multiphysical VCSEL modeling / Tibaldi, A; Gonzalez Montoya, Ja; Bertazzi, F; Goano, M; Debernardi, P. - STAMPA. - (2018), pp. 19-20. (Intervento presentato al convegno 18th International Conference on Numerical Simulation of Optoelectronic Devices (NUSOD 2018) tenutosi a Hong Kong, China nel 05-09 November 2018) [10.1109/NUSOD.2018.8570284].

Availability:

This version is available at: 11583/2728363 since: 2022-07-27T07:55:46Z

Publisher:

IEEE

Published

DOI:10.1109/NUSOD.2018.8570284

Terms of use:

This article is made available under terms and conditions as specified in the corresponding bibliographic description in the repository

Publisher copyright

IEEE postprint/Author's Accepted Manuscript

©2018 IEEE. Personal use of this material is permitted. Permission from IEEE must be obtained for all other uses, in any current or future media, including reprinting/republishing this material for advertising or promotional purposes, creating new collecting works, for resale or lists, or reuse of any copyrighted component of this work in other works.

(Article begins on next page)

Bridging scales in multiphysical VCSEL modeling

Alberto Tibaldi*, Jesus Alberto Gonzalez Montoya†, Francesco Bertazzi*†, Michele Goano*†, Pierluigi Debernardi*,
* IEIIT-CNR, Politecnico di Torino, corso Duca degli Abruzzi 24, 10129 Torino, Italy

† Dipartimento di Elettronica e Telecomunicazioni, Politecnico di Torino, corso Duca degli Abruzzi 24, 10129 Torino, Italy
E-mail: alberto.tibaldi@polito.it

Abstract—On our way to develop a multiphysical model of VCSELs including carrier transport, electromagnetic propagation, and heat conduction, we discuss some critical aspects of the adopted multiscale strategy. In particular, we address the inclusion of non-classical corrections within a classical carrier-transport framework, and the possibilities offered by rigorous approaches such as the nonequilibrium Green’s function (NEGF) towards the determination of some critical parameters, bridging from the nanometer to the macroscopic scale. This seems a promising line of action towards the simulation and optimization of 3D highly nanostructured devices such as VCSELs.

Index Terms—VCSELs, carrier transport, optoelectronic device simulation, NEGF

I. INTRODUCTION

A realistic model of vertical-cavity surface-emitting lasers (VCSELs) should address the complex and entangled interplay of carrier transport, optical transitions, electromagnetic propagation, and heat conduction: for efficient current injection, the current-carrying extended states of the system are connected to the localized states populated by carriers interacting with the electromagnetic cavity modes, whose excitation and topography depend on the optical response of the active region. Although VCSELs are admittedly highly nanostructured, they really are three-dimensional macroscopic structures that typically don’t lend themselves to a fully quantum kinetic treatment. Considering the staggering computational cost of quantum kinetic approaches, one viable solution to the modeling of the spatial and temporal dynamics of VCSELs seems to be a drift-diffusion transport approach complemented with appropriate quantum models validated by NEGF tools. The most complete multi-physics VCSEL simulators are probably the ones developed at ETH Zurich [1], [2], later included in Synopsys Sentaurus Device [3], and at Georgia Tech [4], [5]. In an effort to advance in this field, we are currently developing a comprehensive VCSEL electro-opto-thermal numerical simulator. Our multiscale/multiphysics model includes (i) a quasi-3D drift-diffusion code based on an axisymmetric FEM basis to describe vertical carrier transport across the distributed Bragg reflectors (DBRs) and through the oxide-aperture, (ii) quantum corrections in the “quantum” region of the device including a Poisson-Schrödinger solver to account for quantum confinement and rate equations connecting 3D barrier states with 2D quantum well states [6]–[8], with an educated guess of the coupling parameters inspired by nonequilibrium Green’s function (NEGF) simulations of the active region of the VCSEL [9], (iii) a full-wave EM model based on coupled

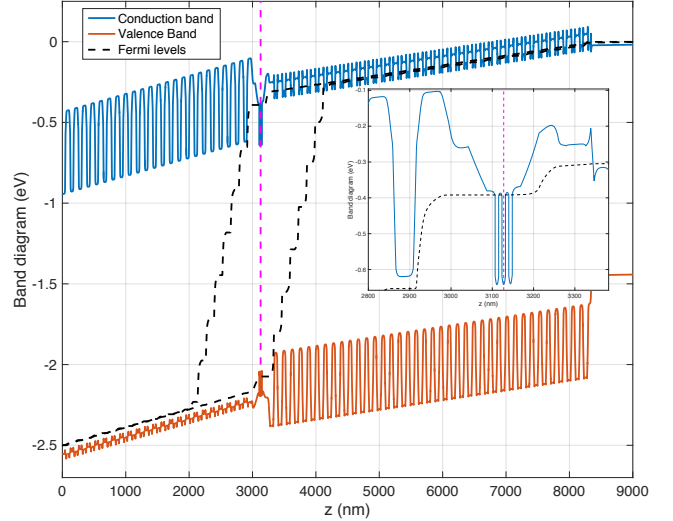


Fig. 1. Band diagram of a GaAs-based VCSEL above turn-on. The active region is just a small portion of the whole device whose position is marked by a dashed vertical line. The inset shows a zoom of the band diagram in the active region, which includes three quantum wells

mode theory, which provides threshold gains and the spatial pattern of cavity modes, complemented with (iv) a material gain model, and (v) a heat transfer model describing the impact of thermal effects on the shift of the lasing wavelength, threshold currents, and optical power. All the above models are iteratively solved until self-consistency is achieved.

II. RESULTS

Carrier transport across the DBRs is one of the most critical ingredients of the VCSEL model [10]. DBRs are graded superlattices constituting the majority of the VCSEL volume, as the band diagram of Fig. 1 clearly shows. Carrier transport across the active region is complemented with photon rate equations to couple the optical modes with the confined populations in the active region and additional drift-diffusion equations to describe the lateral currents in the quantum well plane for the inclusion of spatial hole burning effects, see Fig. 2 for a typical current density distribution. We coupled this “quantum-corrected” DD code to a full-wave electromagnetic solver based on the expansion of the electromagnetic field in terms of the complete basis of the TE and TM modes of the cavity

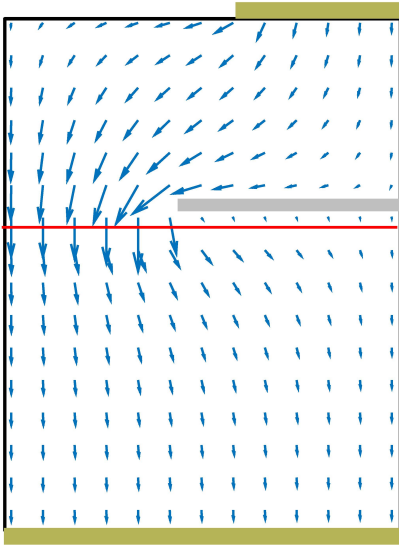


Fig. 2. Vector plot of the current density in a VCSEL.

medium in cylindrical coordinates, where all deviations with respect to the reference unperturbed structure are accounted by coupled-mode theory [11]. (This model has been successfully applied to several advanced VCSEL designs [12]–[15].) The requirement that the solutions of the electromagnetic problem match the optical response of the active region provides a self-consistent mechanism for the selection of the lasing modes.

The modal gain, which couples the carrier transport and optical models, is computed with the Fermi Golden rule (FGR), and validated by means of NEGF simulation. The interactions included in the NEGF approach are carrier-phonon and carrier-photon scattering. All self-energies are fully nonlocal and computed in the self-consistent Born approximation [16]. Inclusion of carrier-carrier interactions beyond the Hartree level is necessary to describe excitonic effects in the optical spectra and will be part of future work. The subband dispersion of the active region shown in Fig. 3 (left) is computed with a multiband $4 \times 4 \mathbf{k} \cdot \mathbf{p}$ approach [17]. The gain/absorption coefficient computed within the NEGF framework (red dashed lines) matches closely the FGR result (blue lines), up to the effects of a finite broadening, which is described by a phenomenological dephasing constant in the FGR approach, see Fig. 3 (right).

The thermal rollover is a crucial effect in VCSEL operation, because it limits the available optical power. This appears to be the most complex phenomenon to be correctly reproduced, because it is ruled by the entangled temperature dependence of the different recombination terms, in particular Auger recombination [18]–[20].

ACKNOWLEDGMENT

This work was supported in part by the U.S. Army Research Laboratory through the Collaborative Research Alliance (CRA) for MultiScale multidisciplinary Modeling of Electronic materials (MSME).

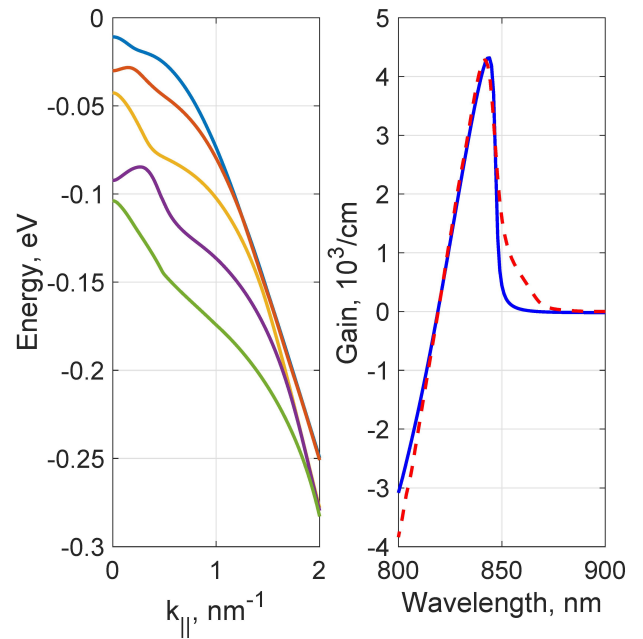


Fig. 3. Left. Subband hole dispersion of a typical active region as a function of the transverse wavevector, computed with a multiband $4 \times 4 \mathbf{k} \cdot \mathbf{p}$ approach. Right. The gain/absorption coefficient computed within the NEGF framework (red dashed lines) matches closely the FGR result (blue lines), up to the effects of finite broadening, which are included in the FGR formalism by means of a phenomenological dephasing constant.

REFERENCES

- [1] B. Witzigmann, A. Witzig, W. Fichtner, *IEEE Trans. Electron Devices* **47**, 1926 (2000).
- [2] M. Streiff, A. Witzig, M. Pfeiffer, P. Royo, W. Fichtner, *IEEE J. Select. Topics Quantum Electron.* **9**, 879 (2003).
- [3] Synopsys, Inc., Mountain View, CA, *Sentaurus Device User Guide. Version M-2016.12* (2016).
- [4] M. M. Satter, P. D. Yoder, *Opt. Quantum Electron.* **42**, 747 (2011).
- [5] K. Mehta, *et al.*, *IEEE J. Quantum Electron.* **54**, 1 (2018).
- [6] M. Grupen, K. Hess, *IEEE J. Quantum Electron.* **34**, 120 (1998).
- [7] M. Vallone, F. Bertazzi, M. Goano, G. Ghione, *J. Appl. Phys.* **121**, 123107 (2017).
- [8] C. De Santi, *et al.*, *Nitride Semiconductor Light-Emitting Diodes*, J. J. Huang, H. C. Kuo, S.-C. Shen, eds. (Woodhead Publishing, Duxford, U.K., 2018), chap. 14, pp. 455–489, second edn.
- [9] F. Bertazzi, *et al.*, *Handbook of Optoelectronic Device Modeling and Simulation*, J. Piprek, ed. (CRC Press, Boca Raton, FL, 2017), chap. 2, pp. 35–80.
- [10] M. Calciati, A. Tibaldi, F. Bertazzi, M. Goano, P. Debernardi, *Semiconductor Sci. Tech.* **32**, 055007 (2017).
- [11] P. Debernardi, G. P. Bava, *IEEE J. Select. Topics Quantum Electron.* **9**, 905 (2003).
- [12] P. Debernardi, R. Orta, T. Gründl, M.-C. Amann, *IEEE J. Quantum Electron.* **49**, 137 (2013).
- [13] A. Tibaldi, *et al.*, *IEEE Trans. Microwave Theory Tech.* **63**, 11 (2015).
- [14] A. Tibaldi, P. Debernardi, R. Orta, *IEEE J. Quantum Electron.* **51**, 2400407 (2015).
- [15] P. Debernardi, *et al.*, *IEEE J. Quantum Electron.* **52**, 2400108 (2016).
- [16] U. Aeberhard, *IEEE J. Select. Topics Quantum Electron.* **19**, 4000411 (2013).
- [17] X. Zhou, F. Bertazzi, M. Goano, G. Ghione, E. Bellotti, *J. Appl. Phys.* **116**, 033709 (2014).
- [18] F. Bertazzi, M. Goano, E. Bellotti, *J. Electron. Mater.* **40**, 1663 (2011).
- [19] F. Bertazzi, *et al.*, *Appl. Phys. Lett.* **106**, 061112 (2015).
- [20] J. Piprek, *IEEE J. Quantum Electron.* **53**, 1 (2017).